A and B-type internal solitary waves in the northern South China Sea.

Vasiliy Vlasenko, Chuncheng Guo, and Nataliya Stashchuk

School of Marine Sciences and Engineering, the University of Plymouth, Drake Circus, Plymouth PL4 8AA

Internal solitary waves (ISWs) in the northern South China Sea (SCS, see Figure 1) are investigated using historical observational data, linear theory, global inverse tidal model, and a fully nonlinear nonhydrostatic numerical model.

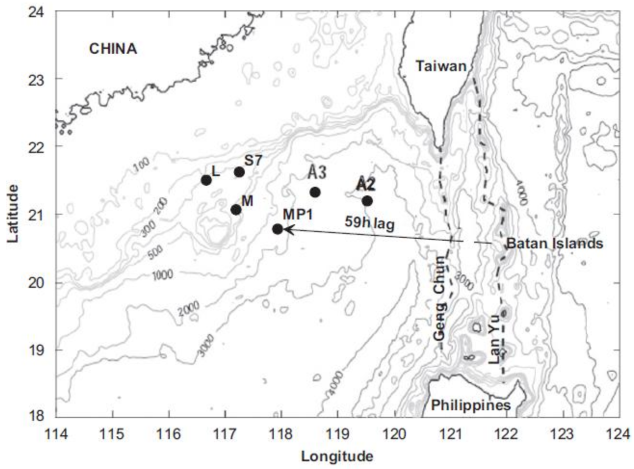

Figure 1. Bottom topography of the north-eastern South China Sea with the positions of moorings L, M, S7, A2, A3 and MP1 discussed in the cited literature (black dots). General direction of ISW propagation is shown by the arrow.

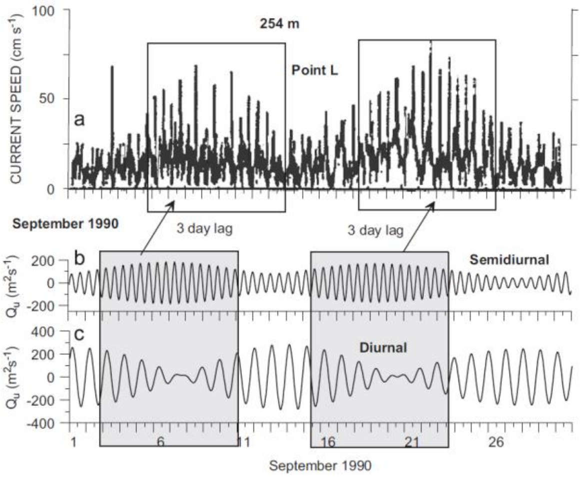

Figure 2. (a) Current speed recorded at 254 m depth at point L in September 1990 (Ebbersmeyer et al., 1991). Panels (b) and (c) show the zonal barotropic water discharge for semidiurnal and diurnal tidal components at the Luzon Strait (LS).

Analysis of all available historical mooring data (an example is presented in Figure 2) shows a very strong correlation between the ISWs observed in the northern SCS and the intensity of the semidiurnal tidal harmonics in the LS. Much stronger diurnal constituents do not reveal any substantial influence on the appearance of ISWs. (see Figure 1). This conclusion on predominantly semidiurnal nature of baroclinic tides in the northern SCS is supported by all published observational data sets and can be explained in terms of the rotational dispersion: production of ISWs in high-latitude seas (the LS is located between 19 and 221N, which is close to the critical latitudes for the diurnal harmonics) is suppressed by the rotation.

The role of the diurnal tidal harmonics lies in the modulation of the generated internal wave fields in such a way that a diurnal periodicity is introduced into the ISW signal known as A- and B-waves. In our study we follow the Ramp et al.(2004) classification calling all large-amplitude rank-ordered ISW packets as A-waves, and single weak ISWs as B-waves. It was found that the appearance of A- or B-type waves is not directly linked to strong or weak tidal current in the LS.

The MITgcm forced by a superposition of all principal tidal harmonics reproduces both types of waves. The numerical experiments conducted for April–May, 2007 and July, 2010 show that the number of ISWs in A- and B-wave packets varies with neap-spring periodicity (see Figure 3). Most clearly this periodicity is seen in a gradual transition of A- waves into B-waves, and B-waves into A-waves. The arrival time of A- and B-waves at any fixed observational point is also not a unique characteristic of any particular type of wave. It varies both for A and B packets depending on the forcing conditions in the LS.

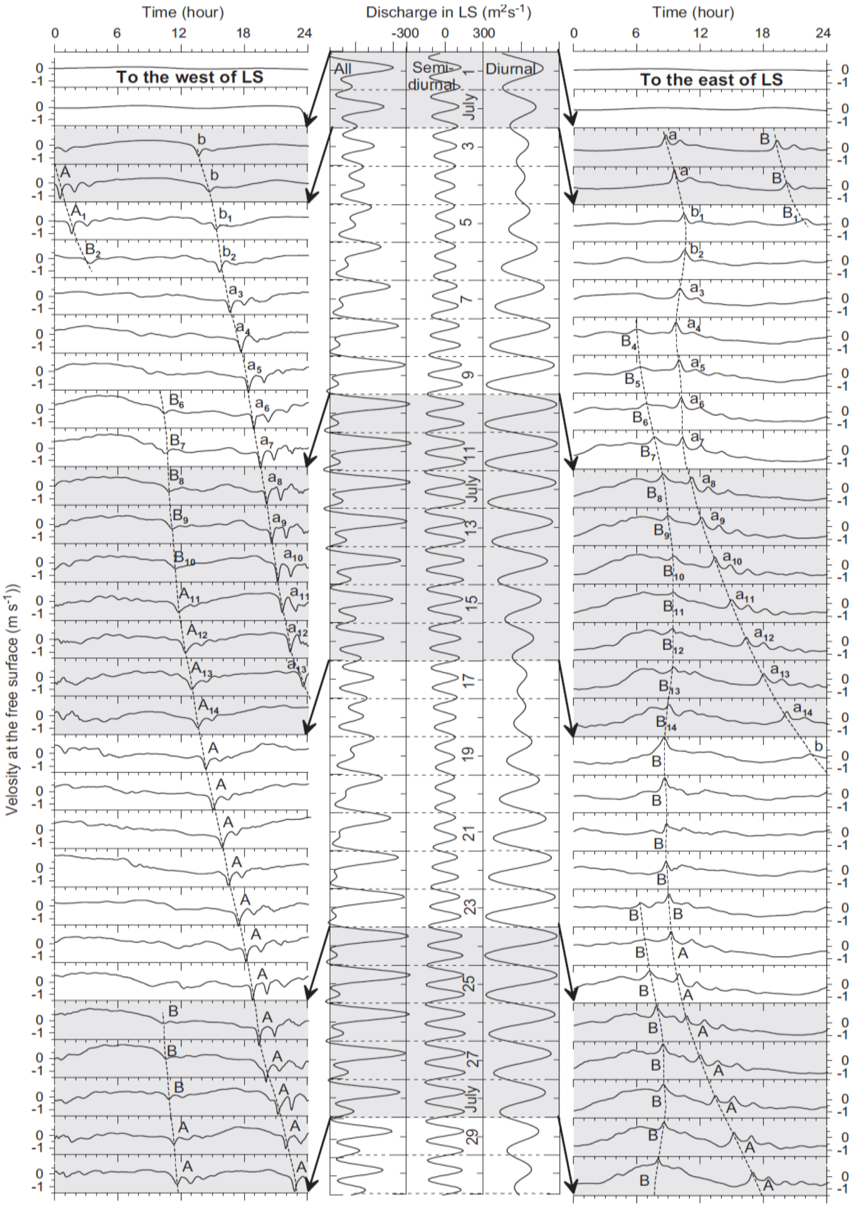

Figure 3. Time series of the horizontal velocity at the free surface 430 km to the west (left column) and 430 km to the east (right column) from the LS for July, 2010. Waves A(a) and B(b) are marked by the appropriate letters. Three graphs in the middle represent east-west discharge predicted by TPXO7.1 for all, semidiurnal and diurnal tidal harmonics (marked accordingly). Arrows show the time lag between tidal forcing in the LS and the signal in the control points.

The effect of A-B-A-B wave transition (see Figure 3) is treated here in terms of a multi-harmonic evolutionary mechanism. Analysis of the generation conditions at the LS supports the idea that tidally generated internal waves freely radiate from the ridge. The radiated waves are a superposition of semidiurnal and diurnal internal tidal harmonics. The amplitudes of the most energetic first-mode internal waves were calculated using the linear theory of tidal energy conversion. Being superimposed, these two progressive waves (semidiurnal and diurnal) produce an intermittent baroclinic signal with large and small wave troughs alternating in space. In the course of nonlinear evolution these large and small wave troughs steepen and ultimately disintegrate into A- and B-wave packets, respectively. Direct comparison of the multi-harmonic wave evolution with the results of the MITgcm modelling revealed a perfect correlation between the types of waves predicted by both methods.

References:

Ebbersmeyer, C.C., Coomes, C.A., Hamilton, R.C., Kurrus, K.A., Sullivan, T.C., Salem B.L., Romea, R.D., Bauer, R.J., 1991. New observations on internal waves (solitons) in the South China Sea using an acoustic Doppler current profiler. In: Proceedings of Marine Technology Society Conference, New Orleans, May 1991, pp. 165–175.

Ramp, S.R., Tang, T.Y., Duda, T.F., Lynch, J.F., Liu, A.K., Chiu, C.-S., Bahr, F.L., Kim, H.-R., Yang, Y.-J., 2004. Internal solitons in the northeastern South China Sea. Part I: Sources and deep water propagation. IEEE J. Ocean. Eng. 29 (4), 1157–1181.